J Biomol NMR (2011) 50:71–81
DOI 10.1007/s10858-011-9495-3

ARTICLE

Fast methionine-based solution structure determination of calcium-calmodulin complexes

Jessica L. Gifford · Hiroaki Ishida · Hans J. Vogel

Received: 23 December 2010 / Accepted: 16 February 2011 / Published online: 1 March 2011

Abstract Here we present a novel NMR method for the structure determination of calcium-calmodulin (Ca^{2+}-CaM)-peptide complexes from a limited set of experimental restraints. A comparison of solved CaM-peptide structures reveals invariability in CaM's backbone conformation and a structural plasticity in CaM's domain orientation enabled by a flexible linker. Knowing this, the collection and analysis of an extensive set of NOESY spectra is redundant. Although RDCs can define CaM domain orientation in the complex, they lack the translational information required to position the domains on the bound peptide and highlight the necessity of intermolecular NOEs. Here we employ a specific isotope labeling strategy in which the role of methionine in CaM-peptide interactions is exploited to collect these critical NOEs. By ^{1}H, ^{13}C-labeling the methyl groups of deuterated methionine against a ^{2}H, ^{12}C background, we can acquire a ^{13}C-edited NOESY characterized by simplified, easily analyzable spectra. Together with measured CaM backbone H_N-N RDCs and intrapeptide NOE-based distances, these intermolecular NOEs provide restraints for a low temperature torsion-angle dynamics and simulated annealing protocol used to calculate the complex structure. We have applied our method to a CaM complex previously solved through X-ray crystallography: Ca^{2+}-CaM bound to the CaM kinase I peptide (PDB code: 1MXE). The resulting structure has a backbone RMSD of 1.6 Å to that previously published. We have also used this test complex to investigate the importance of homologous model selection on the calculated outcome. In addition to having application for fast complex structure determination, this method can be used to determine the structures of difficult complexes characterized by chemical shift overlap and broad signals for which the traditional method based on the use of fully ^{13}C, ^{15}N-labeled CaM fails.

Keywords Calmodulin · Calmodulin complex · Methionine labeling · Methyl labeling · Residual dipolar couplings · Structure determination

Introduction

In eukaryotic cells, the calcium (Ca^{2+}) cation is a crucial secondary messenger and calmodulin (CaM) is its primary protein mediator (Chin and Means 2000; Vogel 1994). Expressed in all cell types CaM is a small, highly α-helical, bilobal protein in which the independently folded N- and C-terminal globular domains are connected by a highly flexible linker (Barbato et al. 1992; Tjandra et al. 1995). A member of the EF-hand superfamily, each domain of CaM contains two helix-loop-helix Ca^{2+} binding motifs (Gifford et al. 2007). Upon binding four Ca^{2+} cations through these motifs, CaM undergoes a conformational change that allows it to bind and activate well over 350 distinct target proteins (Hoeflich and Ikura 2002; Ishida and Vogel 2006; Yamniuk and Vogel 2004; Yap et al. 2000). The scope of binding partners is impressive as targets include proteins involved in phosphorylation/dephosphorylation events, cell signaling, the cytoskeleton, as well as various ion channels and receptors. The importance of CaM is seen in its strictly conserved amino acid sequence which is invariant among

Electronic supplementary material The online version of this article (doi:10.1007/s10858-011-9495-3) contains supplementary material, which is available to authorized users.

J. L. Gifford · H. Ishida · H. J. Vogel (✉)
Biochemistry Research Group, Department of Biological Sciences, University of Calgary, Calgary, AB T2N 1N4, Canada
e-mail: vogel@ucalgary.ca

vertebrate species and by the fact that deletion of the CaM gene in yeast is lethal (Davis et al. 1986).

Structurally, Ca^{2+} binding causes helical rearrangement in both domains of CaM leading to the exposure of large hydrophobic amino acid side chains that are buried in the apo form (Zhang et al. 1995). This creates an extensive hydrophobic patch on each domain through which Ca^{2+}-CaM interacts with the primarily hydrophobic CaM-binding domains of its target proteins. Besides common motifs for the spacing of hydrophobic amino acid side chain anchors, there is no consensus sequence among the Ca^{2+}-CaM-binding domains. How CaM is able to bind to and regulate many target proteins without relying on the presence of a specific amino acid sequence in its binding partners is attributed to two characteristics. The first is the flexibility of the central linker which enables the two globular domains to adopt a number of binding orientations. The second is the high number of methionine residues found in the exposed hydrophobic patches: four in each domain making up nearly half of the hydrophobic surface area of each patch (Fig. 1) (Ishida and Vogel 2006; Yamniuk et al. 2009).

The high number of methionines in CaM (9 out of 148 amino acid residues) is uncommon in proteins and is tied to CaM's function. The methionine side chain has unique chemical and physical properties that make it an ideal group for creating a malleable nonpolar binding surface. As dispersion forces contribute significantly to the net attraction between nonpolar binding partners, the substantially larger polarizability of sulfur compared to typical hydrocarbon moieties makes this side chain especially "sticky" (Gellman 1991). Furthermore, the long flexible side chain enables the hydrophobic patches to be highly conformationally adaptable (Gellman 1991; Siivari et al. 1995). This flexibility, as compared to leucine or isoleucine, is not exclusively the result of differences in branching as, due in part to the presence of sulfur, the side chain exhibits little enthalpic preference between gauche or anti χ_3 torsion angles allowing the terminal methyl group to mold into various nonpolar binding surfaces. More than any other type of amino acid in CaM's exposed hydrophobic patches, the methionine side chains, in particular the terminal ε-methyl groups, are directly involved in target binding (Zhang et al. 1994; Lee et al. 2000; Siivari et al. 1995; Yuan et al. 1999, 2004; Ishida and Vogel 2006) and their presence has been shown through mutant-based studies to be essential (Zhang and Vogel 1994; Edwards et al. 1998; Chin and Means 1996).

Structural studies of CaM-target protein interactions typically use short peptide sequences comprising CaM-binding domains. This practice reflects both the size limitation of traditional NMR methods and the fact that crystallization of intact complexes has been largely unsuccessful. Fortunately, the applicability of peptides to represent intact CaM-binding domains is supported by various studies including mutagenic (Chin et al. 1997), spectroscopic (Gomes et al. 2000), TROSY-based NMR (Kranz et al. 2002), and SAXS (Krueger et al. 1997). In this manner, several structures of complexed CaM have been solved and a comparison of these structures highlights the fact that it is predominantly the orientation of CaM's two domains that adjusts between the different complex structures and not the overall structure of CaM itself [for a review see Ishida and Vogel (2006)]. In particular, there is a high degree of similarity in the backbone conformation between the various structures [0.88 and 0.67 Å backbone RMSD for the N- and C-lobes of CaM respectively when select complexes are compared including the divergent GAD, edema factor, SK channel and Nap-22 complexes (Ishida and Vogel 2006)]; CaM appears to rely on highly flexible amino acid side chains as well as the central linker to adopt to divergent target sequences.

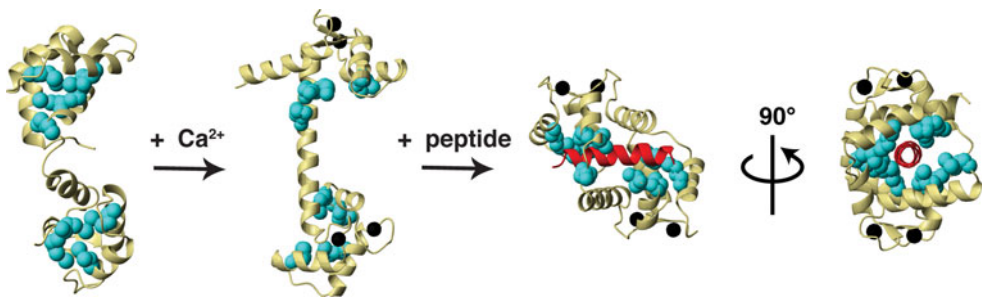

Fig. 1 The role of methionine in CaM target interactions. From left to right the structures are: apo-CaM, Ca^{2+}-CaM, Ca^{2+}-CaM in complex with the smMLCKp peptide, and its 90° *y*-axis rotation (PDB codes 1DMO, 1CLL, 1CDL respectively). In each structure CaM is colored *yellow*, the bound target peptide is colored *red*, the Ca^{2+} atoms are colored *black*, and the critical methionine side chains are shown in *blue* space-fill representation with their importance in target binding clearly seen in the complex structures. Eight out of CaM's nine methionines are located in the hydrophobic patches of the two domains: methionines 36, 51, 71, and 72 are located in the N-terminal patch (oriented on top), 109, 124, 144, 145 are located in the C-terminal patch (oriented on bottom), and 76 is located in the central linker

Here we present a method for relatively quick NMR-based structure determination of Ca^{2+}-CaM complex structures. Knowing there is little variation in the backbone conformation of CaM complexes, there is no need to collect and analyze an extensive set of NOE-based experiments to in turn define the structure of CaM, the bound peptide, and the binding interface. Instead, a more direct approach can be used through which RDC analysis provides information on the domain orientation of CaM and intermolecular NOEs between the bound peptide and CaM supply the domain translational information not provided by RDCs. To collect the critical intermolecular NOEs we have employed an isotope labeling strategy in line with the popular approach of ^{1}H, ^{13}C-labeling the methyl groups of Ile, Leu and Val against a perdeuterated background (Ruschak and Kay 2010; Otten et al. 2010). By methyl-labeling the otherwise deuterated methionines in CaM we can collect intermolecular NOEs between these methyl groups and protons in the bound peptide. Furthermore, this labeling strategy produces simplified, easily analyzable spectra with both increased sensitivity and resolution.

We have applied this method to a CaM complex previously solved through X-ray crystallography: Ca^{2+}-CaM bound to a peptide from CaM kinase I (CaMKI) (PDB code 1MXE) (Clapperton et al. 2002). CaMKI, along with CaMKK and CaMKIV comprise the CaM-dependent kinases signaling cascade thought to play a critical role in neuronal development, plasticity and behavior (Soderling 1999; Wayman et al. 2008). Our resulting structure has a backbone RMSD of 1.6 Å to that published. Furthermore we have investigated the importance of choosing the correct starting model both in terms of homologous CaM domain orientation as well as the correct direction of the bound peptide.

Experimental procedures

Sample preparation

CaM was overexpressed and purified from *Escherichia coli* BL21(DE3) cells containing the ET30b(+) expression vector. This study required three isotopically enriched versions of CaM. For the standard backbone and side chain assignment of CaM in the complex uniformly $^{13}C/^{15}N$-labelled CaM was prepared in M9 media containing 0.5 g/l $^{15}NH_4Cl$ and 3 g/l [$^{13}C_6$]glucose. To determine the structure of the bound CaMKI peptide uniformly $^{2}H/^{15}N$-labelled CaM was prepared in 99.9% D_2O based M9 minimal media containing 0.5 g/l $^{15}NH_4Cl$ and 4 g/l [$^{2}H_7$]glucose. Finally, intermolecular NOEs between CaM and the CaMKI peptide were obtained using a methionine methyl-labeled version of otherwise fully deuterated ^{15}N-labelled CaM. ($^{1}H/^{13}C$-methyl-Met)/$^{2}H/^{15}N$ CaM was created by supplementing 100 mg/l of ^{1}H-α,ε- ^{13}C-ε- ^{2}H-methionine to 99.9% D_2O M9 media containing 0.5 g/l $^{15}NH_4Cl$ and 4 g/l [$^{2}H_7$]glucose 1 h prior to induction with IPTG, a procedure analogous to that used to make Ile/Leu/Val-methyl protonated (but otherwise fully deuterated) protein (Tugarinov et al. 2006). ^{1}H-α,ε- ^{13}C-ε- ^{2}H-methionine was synthesized from methyl-^{13}C iodide and (3,3,3′,3′,4,4,4′,4′-$^{2}H_8$)-DL-homocystine (Cambridge Isotopes) according to a previously published protocol (Melville et al. 1947) except that the neutralization was performed with hydrobromic acid. The identity as well as isotope-labeling pattern of this methionine was confirmed using 1D NMR. All versions of CaM were purified to homogeneity by Ca^{2+}-dependent phenyl Sepharose column chromatography as previously described (Yuan et al. 1999; Zhang and Vogel 1993, 1994).

The CaMKI peptide (CaMKIp) (Ac-AKSKWKQAF-NATAVVRHMRKLQ-NH_2) corresponding to residues 299–320 of CaM kinase I in rat brain (Goldberg et al. 1996) was commercially synthesized (Anaspec) and determined to be more than 95% pure by matrix-assisted laser desorption/ionization mass spectroscopy and high pressure liquid chromatography.

Samples for NMR spectroscopy contained 638–950 μM $^{13}C/^{15}N$, $^{2}H/^{15}N$, or ($^{1}H/^{13}C$-methyl-Met)/$^{2}H/^{15}N$ CaM in 20 mM Bis–Tris (pH 6.8), 100 mM KCl, 4 mM $CaCl_2$, 0.03% NaN_3, 0.5 mM 2,2-dimethyl-2-silapentane-5-sulfonate and either 90% H_20/10% D_2O or 99.9% D_2O. Complexes between CaM and CaMKIp were created with either an excess of peptide (1.1:1 and 1.3:1 molar ratio with $^{13}C/^{15}N$ or ($^{1}H/^{13}C$-methyl-Met)/$^{2}H/^{15}N$ CaM, respectively) or an excess of CaM (0.6:1 molar ratio with $^{2}H/^{15}N$ CaM) depending on the purpose of the NMR sample. The sample used for RDC measurements contained an extra 200 mM KCl and 16 mg/ml filamentous phage Pf1 (Asla Biotech Ltd.) to achieve partial alignment.

NMR spectroscopy

All NMR experiments for structure determination were performed at 30°C on a Bruker Avance 500-MHz NMR spectrometer equipped with a triple resonance inverse Cryoprobe with a single axis z-gradient. Resonance assignments of H_N, N, C′, C_α and C_β for CaM in the complex were obtained from the BioMagResBank (BMRB number 5286) (Kranz et al. 2002) and confirmed using two-dimensional [^{15}N-^{1}H]-HSQC and three-dimensional CBCA(CO)NH, HNCACB, HNCO, and HN(CA)CO experiments. Side-chain assignments were defined through the three-dimensional experiments C(CCO)NH TOCSY, H(CCO)NH TOCSY and HBHA(CBCACO)NH. For the methionine side chain methyl group assignments

three-dimensional HMBC and LRCH experiments that record the long-range correlations between the Hε/Cε and Hγ/Cγ atoms were used (Bax et al. 1994). Resonance assignments as well as intrapeptide NOEs for CaMKIp in complex with $^{2}H/^{15}N$ CaM were obtained from a two-dimensional COSY and a two-dimensional NOESY with an isotope filter in the F2 dimension (Breeze 2000). Intermolecular NOEs between the peptide and ($^{1}H/^{13}C$-methyl-Met)/$^{2}H/^{15}N$ CaM were obtained through a three-dimensional NOESY-[^{13}C-^{1}H]-HSQC. All NOESY experiments for the structure determination of this complex were measured with a mixing time of 100 ms. $^{1}D_{NH}$ RDCs were measured using an IPAP-HSQC (Ottiger et al. 1998) with 2,048 × 512 complex points. After linear prediction and zero filling the digital resolution was 1.2 Hz/pt in the ^{15}N dimension. ^{1}H, ^{13}C, and ^{15}N chemical shifts in all spectra were referenced using 2,2-dimethyl-2-silapentane 5-sulfonate as previously described (Wishart et al. 1995). Spectra were processed with the NMRPipe package (Delaglio et al. 1995) and analyzed using NMRView (Johnson and Blevins 1994). The resonance assignments for the bound peptide as well as the methionine methyl groups of calmodulin in complex have been deposited in the BMRB database under accession number BMRB-17360.

Structure calculation

Initial homologous model selection for the structure calculation was determined through singular value decomposition using the PALES software (Zweckstetter and Bax 2000) a program which fits the measured CaM H_N-N RDCs from our complex to those back-calculated from crystal structures of other CaM:peptide complexes deposited in the Protein Data Bank (PDB). Only structured regions of CaM were chosen for analysis: residues 6–72 from the N-terminal domain and 85–144 from the C-terminal domain (Mal et al. 2002). CYANA (version 2.0) was used to assign the CaMKIp intrapeptide NOEs in the complex and determine the bound peptide's structure (Guntert 2003). The resulting peptide structure was then used to derive upper distance limit restraints as well as hydrogen bonding and backbone dihedral angle restraints. CaM-specific restraints included H_N-N RDCs, hydrogen bond restraints based on chemical shift index derived secondary structure prediction, backbone dihedral angle restraints obtained from both the starting model and predicted by TALOS (Chou et al. 2000; Cornilescu et al. 1999) and Ca^{2+} ligand restraints. Finally, the intermolecular NOEs observed between CaM methionine methyl groups and the peptide were all binned into one distance class of 1.8–6.0 Å. Due to the lack of a suitable internal standard through which to calibrate the NOESY-[^{13}C-^{1}H]-HSQC spectrum, peak overlap, and the non-linear intensity of potential methyl-methyl NOEs, the NOEs were not classified into bins defined by interatomic distances as a function of peak volume.

Structures were calculated using torsion angle simulated annealing in the program Xplor-NIH (version 2.24) (Schwieters et al. 2003) according to a previously established two step, low temperature protocol (Chou et al. 2000) In the first step, the starting model built from the homologous crystal structure sequentially undergoes Powell energy minimization, 10 ps of torsion angle dynamics at 200 K followed by 4 ps of simulated annealing in which the temperature is decreased from 200 to 20 K in $\Delta T = 10$ K steps. During the simulated annealing the various force constants are ramped up as is standard in Xplor-NIH except the backbone torsion angle restraints for φ and ψ are enforced by a strong harmonic quadratic potential fixed at 300 kcal mol^{-1} rad^{-2}. 100 structures are generated in step 1 and the lowest energy structure is selected as the starting model for step 2. In the second step of the protocol the structure from step 1 undergoes 10 ps of torsion angle dynamics at 20 K which is followed by 6 ps of simulated annealing in which the temperature is decreased from 20 to 1 K in $\Delta T = 1$ K steps. At this point in the calculation the various force constants are held at their final value from step 1 except the backbone dihedral angle force constant for φ and ψ which is ramped down from 300 to 50 kcal mol^{-1} rad^{-2}. Unlike in the first step where unless the TALOS prediction differs by more than 30° in φ and/or ψ the CaM backbone dihedrals are derived from the starting model, in the second step all backbone angle restraints are derived from the lowest energy structure obtained in step 1. 100 structures were generated in step 2 and the lowest energy structure was selected for further analysis including structure validation using the program PROCHECK (Morris et al. 1992). All molecular graphics were created using MOLMOL (Koradi et al. 1996).

Results and discussion

For Ca^{2+}-CaM complexes the importance and role that methionine plays in target binding can be exploited and combined with the use of backbone RDCs to create a faster structure determination protocol. First, H_N-N RDCs are used to select from the PDB a homologous starting structure of CaM in the complex. Then, a specifically labeled version of methionine is used through which intermolecular NOEs between CaM and the bound peptide are obtained.

Homologous model selection

As RDCs are a function of the orientation of interatomic vectors relative to the molecular alignment tensor (Tjandra

et al. 1997), the small exquisitely sensitive one-bond H_N-N RDC can be used to define this bond vector with respect to the external magnetic field and hence the domain orientation of CaM in the complex. H_N-N RDCs have been used successfully to classify CaM-bonding motifs both inside (Mal et al. 2002) and outside the protein kinase family (Contessa et al. 2005). They have also been used in a manner analogous to our approach: to find a homologous complex to serve as a model structure (Scheschonka et al. 2008), or as the starting model in structure calculation refinement (Chou et al. 2000) In the present work, the correlations between 115 measured H_N-N RDCs from CaM in complex with CaMKIp and theoretical RDCs back calculated from crystal structures deposited in the PDB were determined (Table 1, Supplementary Figure S1). As resolution is important only those crystal structures with a resolution of 2 Å or higher were chosen for analysis. Expectedly, the closest agreement is between the measured H_N-N RDCs and the back-calculated values from the crystal structure of CaM:CaMKIp itself (PDB code 1MXE), however, it is not a perfect fit (Supplementary Figure S1). Potential reasons for this are discussed below. The second best agreement between the measured and calculated values is to the CaM complex structure with smMLCKp (PDB code: 1QTX). This published structure was used as the starting model for CaM in our complex.

Bound peptide structure determination

To determine the structure of a bound peptide there are two options. The first is to recombinantly express the peptide in isotope-enriched media enabling the use of standard triple resonance experiments. The second is to use a synthetic unlabeled peptide and homonuclear experiments, an approach that requires isotope filters to select against signals from CaM. If the peptide under study binds strongly to CaM and is of a reasonable length (<30 amino acids) this second approach is most appealing due to the small number of experiments required: only two, a COSY and NOESY (both F1/F2-^{13}C, ^{15}N filtered) as opposed to the swath of backbone, side chain, and NOE-based experiments for a recombinantly labeled peptide. Furthermore, if deuterated CaM is employed in which all but the H_N protons of CaM have been replaced with deuterons in a H_2O-based sample, the more sensitive unfiltered COSY and F2-^{13}C, ^{15}N filtered NOESY can be used.

In this study the second approach has been followed. Using perdeuterated CaM and these two experiments we have assigned the bound CaMKI peptide's proton resonances. Furthermore, inter-residue NOEs observed in the NOESY experiment provide structural information on the bound peptide. Out of a total 353 NOE cross peaks picked in the F2-isotope filtered NOESY, 350 were assigned through the automatic assignment and structure calculation program CYANA (version 2.0) giving a total of 282 non-degenerate NOEs (Table S1 of Supplementary Material). The 20 lowest energy structures calculated using intra-peptide NOEs as well as hydrogen bonding restraints have a backbone RMSD of 0.29 Å (Supplementary Figure S2). The lowest energy structure is α-helical over residues 302–319. As identified by the crystal structure, the two hydrophobic residues that bury deeply into the methionine-rich pockets of CaM (Trp303 and Met316) are pointed in opposite directions away from the peptide. This facilitates the binding of the two domains of CaM.

The CaMKIp structure generated by CYANA was not used in the next steps of the complex structure calculation. However, upper distance restraints resulting from the NOE assignment, hydrogen bonding restraints defined by the α-helical region, as well as backbone dihedral angles from

Table 1 Summary of an H_N-N RDC-based comparison between our solution structure of Ca^{2+}-CaM-CaMKIp and select known CaM complex crystal structures

Complex	Peptide orientation	Binding mode	*R*	*Q* (%)
IMXE:CaMKI	Antiparallel	1–14	0.98	21
1QTX:smMLCK	Antiparallel	1–8–14	0.97	24
2F3Y:Ca(v)1.2 Channel	Parallel	1–10	0.96	28
1CDM:CaMKIIa	Antiparallel	1–5–10	0.94	33
1IQ5:CaMKK	Parallel	1–16	0.93	35
1IWQ:MARCKs	Antiparallel	1–3	0.91	42
INIW:eNOS	Antiparallel	1–8–14	0.90	42
2HQW:NMDA receptor	Antiparallel	1–7	0.89	44
2BCX:ryanodine receptor	Antiparallel	1–17	0.89	45
1PRW:CaM	n/a	n/a	0.84	53

The correlation coefficient (*R*) and quality factor (*Q*) of each pairing indicates the degree of agreement between the orientations of the two domains of CaM in the analyzed complexes; a higher *R* value and lower *Q* value indicating a greater degree of alignment

Table 2 Experimental restraints and structural statistics of the lowest energy structure generated in XPLOR-NIH

Experimental restraints used in the complex structure calculation	
Calmodulin	
Backbone dihedral angle restraints	292
Hydrogen bonding restraints	118
$^{1}D_{NH}$ RDCs	115
Ca^{2+} chelation restraints	24
Inter-methionine NOEs	21
CaMKIp	
CYANA-derived intrapeptide upper distance restraints	244
Backbone dihedral angle restraints	42
Hydrogen bonding restraints	26
Intermolecular NOEs	95
PROCHECK Ramachandran analysis of folded regions (%)	
Residues in most favored regions	93.6
Residues in additional allowed regions	6.4
Residues in generously allowed regions	0
Residues in disallowed regions	0

the lowest energy structure were applied as peptide-specific restraints in the complex calculation in XPLOR-NIH (Table 2).

Intermolecular NOE determination

Once the structure of the bound peptide is determined, the next step is to define where on CaM the peptide is binding. Although RDCs describe a molecular alignment tensor from which we can get the orientation of each domain of CaM, they do not provide translational information on the positions of these domains. This information is obtained through the collection of distance restraints in the form of intermolecular NOEs between CaM and the peptide. As CaM: peptide interactions occur predominantly through side chain as opposed to backbone interactions an F1-^{13}C, ^{15}N filtered, NOESY-[^{13}C-^{1}H]-HSQC is typically used to collect intermolecular NOEs (Breeze 2000). Practically however, this experiment is limited in its sensitivity and resolution, which can become a problem if the complex under study is of a weaker affinity. Poor signal to noise and broadened linewidths coupled with lower spectral resolution can lead to difficulties in assigning the NOE cross-peaks. As an unambiguous assignment of these NOEs is critical to providing the distance restraints that will tie the complex together the limitations of this experiment coupled with the often overlapping chemical shifts of the methyl groups leads to difficulty in obtaining this assignment.

To overcome this problem, the role of CaM's methionine residues in target binding have been exploited to provide probes from which intermolecular NOEs between CaM and the bound peptide can be collected. By endogenously adding ^{1}H-α,ε- ^{13}C-ε- ^{2}H-methionine to CaM recombinantly expressed in ^{2}H, ^{12}C-based media, the methyl groups of methionine are $^{1}H/^{13}C$-labeled while the rest of CaM contains ^{2}H and ^{12}C. This has three advantages. The first is that due to the lack of protons in CaM an isotope filter is no longer required to select for intermolecular NOEs between CaM and the bound peptide. Instead, a standard NOESY-[^{13}C-^{1}H]-HSQC can be used, a more sensitive experiment that increases the signal to noise ratio of the resulting spectra. The second advantage provided by this labeling scheme is an increased resolution in the indirectly detected ^{1}H dimension (F1). Since the only carbon chemical shifts recorded in the ^{13}C dimension (F2) originate from the methionine methyl carbons, the spectral width required to capture these shifts is much smaller: 4 ppm as compared to the approximately 30 ppm needed to encompass the aliphatic carbons in CaM. This smaller window in the ^{13}C dimension enables more points to be collected in the indirectly detected ^{1}H dimension for a similar total experimental time. As an aside, due to the intervening sulfur atom and corresponding weak scalar coupling between the Cε and the Cγ, high resolution data can be obtained if required in the carbon dimension without the use of a constant time experiment. Finally, methionine methyl-labeling produces much simplified spectra. Examples of the [^{13}C-^{1}H]-HSQC spectra of ($^{1}H/^{13}C$-methyl-Met)/$^{2}H/^{15}N$ CaM bound to CaMKIp (Supplementary Figure S3A) and NOESY-[^{13}C-^{1}H]-HSQC strips for M71 and M124 of CaM (Fig. 2) are provided. From eight methionine methyl probes (M76 seems to be free in solution) 95 intermolecular NOEs were observed between these groups and the protonated peptide (Supplementary Figure S3B). In addition to these intermolecular NOEs, several inter-methionine NOEs were also observed (Table 2). This is to be expected due to the close sequential proximity of the methionines (in two instances they are neighbor residues) as well as their spatial proximity seen in other CaM: peptide complexes. Furthermore, weak intra- and inter-residue NOEs are also seen from some methionine methyl groups back to the backbone H_{α}, a proton remaining from the synthesis protocol. Protonation of the methionine at this position provides an extra distance restraint for the calculation and could be used to supplement the methyl assignment obtained via the LRCH experiment.

Structure calculation: 1QTX starting model

As there are no NOE-based restraints to define CaM in the complex, our structure calculation follows a two step low temperature simulated annealing protocol first outlined by Chou et al. (2000). In this protocol a starting model

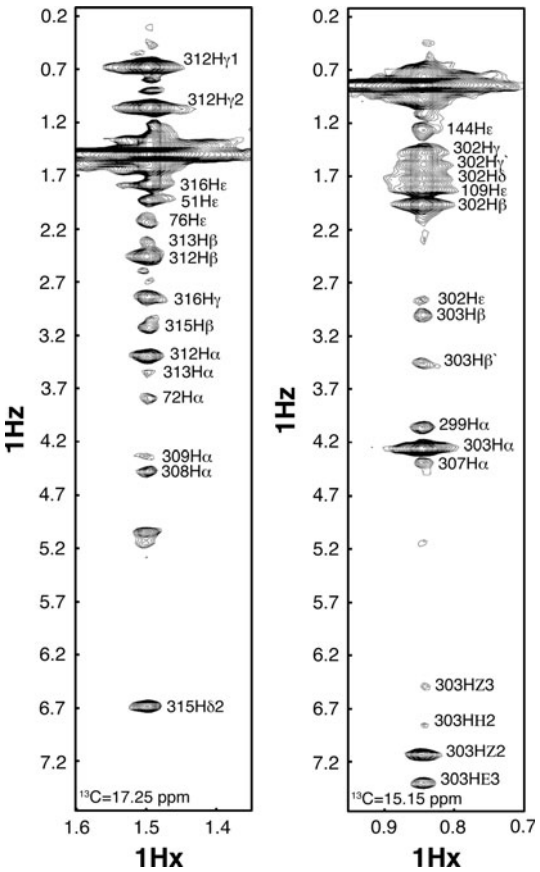

Fig. 2 Unambiguous intermolecular NOEs between CaM and CaMKIp are required to define the peptide-binding interface and provide CaM domain translation information not available from RDCs. By adding $HO^{12}_2C^{12}CH(^{14}NH_2)^{12}CD^{12}_2CD_2S^{13}CH_3$ exogenously to D_2O-based M9 media, recombinant CaM was methyl-labeled on its nine methionines through which these intermolecular NOEs are collected. Shown are representative strip plots from a NOESY-[^{13}C-^{1}H]-HSQC on (^{1}H/^{13}C-methyl-Met)/^{2}H/^{15}N CaM:CaMKIp. The intermolecular NOEs between the methyl groups of M71 (*left*) and M124 (*right*) and identified protons on CaMKIp are indicated

provided by a homologous structure is refined using experimentally measured CaM backbone RDCs and dihedral angle restraints, peptide-specific CYANA-derived distance and angle restraints, and intermolecular NOEs (Table 2). Furthermore, the calculation is distinguished by two adjustments from the normal torsion angle dynamics/simulated annealing protocol in XPLOR-NIH (Schwieters et al. 2003). The first is that it is performed at low temperature: the torsion angle dynamics step occurs at 200 K. This is an important adjustment as there are no restraints except for the intermolecular NOEs to keep the secondary structure elements of CaM together. The second modification is an increased time step for the simulated annealing: up to 30 times longer than in the standard protocol. The length of these time steps is important as the low temperature results in a system with low kinetic energy and longer times are required to allow the system to make the necessary adjustments.

The Ca^{2+}-CaM:CaMKIp complex structure determined through this method is shown in Fig. 3 with structural statics in Table 2. The atomic coordinates have been deposited in the RCSB database under accession number 2L7L. As there is an X-ray crystal structure of this complex deposited in the PDB (PDB code 1MXE) (Clapperton et al. 2002) we can make a comparison with our structure. Not surprisingly the structures are identical both in terms of CaM domain organization as well as the mode of peptide binding: the CaMKI peptide is bound in an antiparallel manner with the N-lobe of CaM binding the C-terminal half of the peptide and the C-lobe of CaM binding the N-terminal half of the peptide, CaMKIp residues Trp303 and Met316 serve to anchor the C- and N-terminal lobes of CaM respectively. Compared to 1MXE our structure has a 1.6 Å backbone heavy atom RMSD over the entire structure, peptide included (Fig. 3b). On a domain specific basis the C-lobes of the two structures are in very good agreement with a backbone RMSD of 1.0 Å; the N-lobe is slightly more divergent as there is a 1.5 Å RMSD. This deviation is small and is possibly explained by the difference in length of the two CaMKI peptides studied, as our peptide is two amino acids longer at the C-terminal end. Of course, in the discrepancy between our structure and 1MXE also lies the difference between a solution and a crystal structure. Evidence for this is seen in the correlation between our measured H_N-N RDCs and the best-fit back-calculated RDCs from 1MXE (Table 1, Supplementary Figure S1). There is not a perfect correlation, in fact the quality factor (*Q*-factor) of this pairing is not much better than that of the Ca^{2+}-CaM:smMLCKp complex (1QTX) (21% as compared to 24%).

Structure calculation: starting model selection

Finally we have investigated any bias introduced into the calculated structure from the starting model. Two new starting models were tested: Ca^{2+}-CaM bound to a peptide from the NMDA receptor (NR1C1p; PDB code 2HQW) and Ca^{2+}-CaM bound to a peptide from CaMKK (CaMKKp; PDB code 1IQ5). Both have divergent domain orientations with respect to the measured H_N-N RDCs (the *Q*-factors for 2HQW and 1IQ5 are 44 and 35% respectively: Table 1, Supplementary Figure S1); the bound peptide is oriented in the correct antiparallel direction in the 2HQW structure but is bound parallel in 1IQ5. Using the 2HQW-derived starting structure, we found that if the starting structure has the correct peptide orientation, by applying our experimental restraints, in particular the RDCs, the structure calculation protocol can reorient the two lobes into the correct position (Fig. 4a). The Ca^{2+}-CaM:CaMKIp structure determined using the 2HQW-derived starting structure has a 1.7 Å

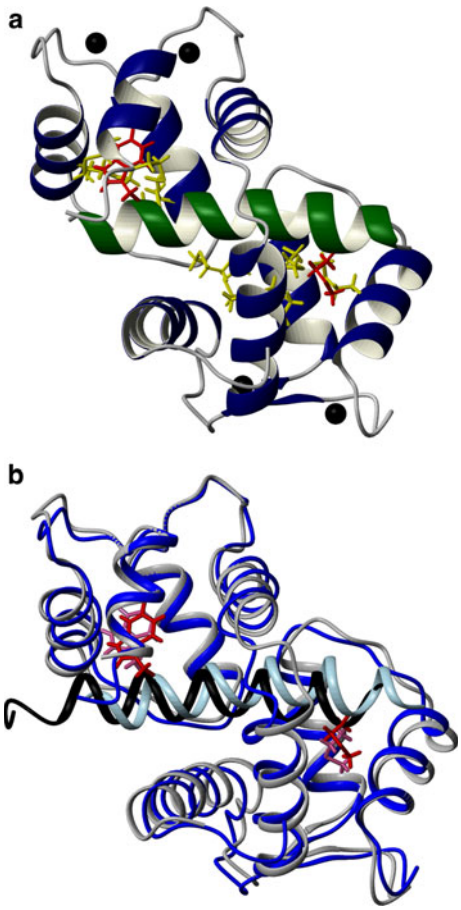

Fig. 3 Complex structure of Ca^{2+}-CaM:CaMKIp. **a** Ribbon representation of the solution structure of Ca^{2+}-CaM bound to CaMKIp. CaM is highlighted in *blue* with the critical methionine side chains indicated in *yellow*, the peptide is colored *green* with its anchor residue side chains Trp303 and Met316 in *red*, and the Ca^{2+} ions are represented by *black spheres*. **b** Backbone overlay of our CaM:CaMKIp structure and the published crystal structure (1MXE). Our structure is highlighted in *blue* for CaM, *light blue* for the peptide with the peptide's anchor residues' side chains shown in *red*. The crystal structure is represented in *grey* for CaM, *black* for the peptide with the anchor residues' side chains in *dark pink*

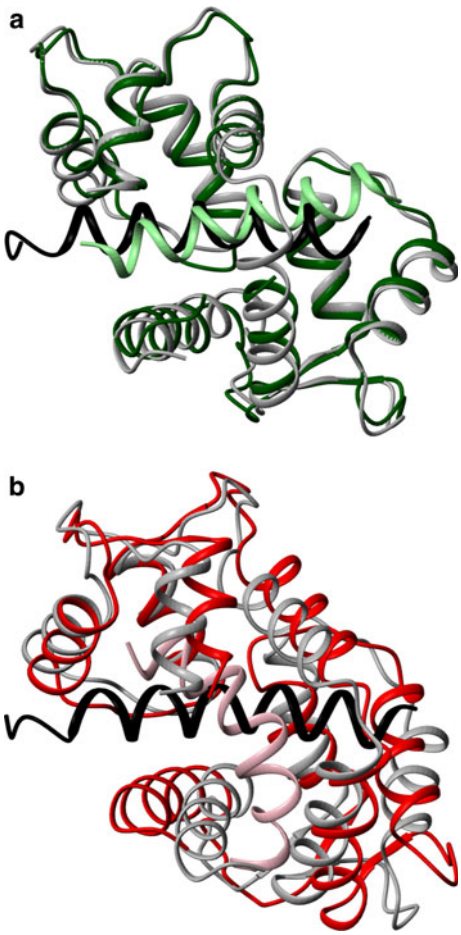

Fig. 4 Overlays of calculated CaM:CaMKIp structures based on two different starting models. The starting model structures tested were complexes of Ca^{2+}-CaM with: **a** NR1C1p (2HQW) and **b** CaMKKp (1IQ5). In each overlay the crystal structure of CaM:CaMKIp is shown in *grey* for CaM, *black* for the peptide. For the calculated structures the backbone as either *green/light green* (NR1C1p-based) or *red/pink* (CaMKKp-based) for CaM and the peptide respectively

backbone RMSD to the 1MXE crystal structure. An even lower 1.3 Å backbone RMSD was observed to the 1QTX-derived solution structure of this complex presented above, indicating a good agreement between the structures calculated using different starting models. A different outcome was found when the 1IQ5-derived starting model was used. Following refinement with the experimentally determined restraints, our finalized structure had a backbone RMSD of 4.9 Å to the 1MXE crystal structure and a similar 4.8 Å RMSD to our 1QTX-derived structure from above (Fig. 4b). Although the supplied H_N-N RDC restraints are satisfied, there is a substantial number of intermolecular NOE violations. Furthermore, upon examination of an overlay of this structure and the 1MXE crystal structure it becomes apparent that the calculation cannot flip the bound peptide into the correct orientation as although several of the intermolecular NOEs are satisfied the peptide has only moved into a vertical position. Even with the addition of a second set of CaM RDCs ($C_\alpha H_\alpha$) we saw no improvement on the agreement between the calculated structures (results not shown).

From these two test cases we can conclude that in terms of homologous model selection, it is more important to choose a starting model with the peptide bound in the correct direction (parallel/antiparallel) than one with optimal CaM domain orientation. Due to the low temperature the calculation is performed at, the structure determination protocol most likely does not have the kinetic energy to flip the bound peptide's orientation. As a consequence, information on the orientation of the peptide is required to assist in the starting model selection. Intermolecular NOEs can provide this information and for the CaMKIp complex the

NOE information was sufficient to determine the orientation of the bound peptide (Supplementary Figure S3B), but if additional information is required other biophysical techniques such as fluorescence and near UV spectroscopy, or nitroxide spin-labels can be used (Barth et al. 1998; Yuan et al. 2004; Gomes et al. 2000; Yuan et al. 1998). In addition, visual inspection of the CaM-binding sequence can also provide clues, as there is evidence that the peptide's charge distribution determines the direction of binding (Osawa et al. 1999).

Conclusion

Here we have presented a method for the "fast" structure determination of Ca^{2+}-CaM:peptide complexes. This method is based on the use of backbone H_N-N RDCs to determine the domain orientation of the two lobes of CaM and intermolecular NOEs between CaM's methionine methyl groups and the protonated peptide to define how the oriented domains bind the peptide. The study of CaM and its binding partners remains an expanding area of research: both new complexes as well as novel binding modes continue to be discovered. Furthermore, of the approximate 350 identified complexes (Yap et al. 2000) the structural details of less than 10% are known. As a structure determination protocol this method has two obvious applications. The first is as a truncated procedure for solving Ca^{2+}-CaM:peptide complexes. In the "omics" era, the "need for speed" is ever present and for many complexes simply removing the requirement of assigning both a NOESY-[^{13}C-^{1}H]-HSQC for CaM-specific NOEs as well as an extensive F1-^{13}C, ^{15}N filtered, NOESY-[^{13}C-^{1}H]-HSQC to collect intermolecular NOEs will speed up the structure determination process. The second application is as a method for "difficult" complexes. As the "low hanging fruit" of the Ca^{2+}-CaM complexes disappear many of the undetermined structures are of weaker affinity and fall on the border between slow and intermediate exchange on the NMR time scale. Due to the exchange rate, the key NOESY-[^{13}C-^{1}H]-HSQC spectra (both unfiltered and filtered versions) are characterized by peak broadening which, compounded with the limited resolution of these experiments, makes spectra assignment and thus NOE collection difficult. The presented labeling scheme helps to overcome this limitation, as the collection of NOESY-based spectra with both increased sensitivity and resolution is possible. Furthermore, due to the comparably more favorable relaxation rates of the methyl group of the methionine side chain, this group should be less affected by the peak broadening produced by either chemical exchange or decreased molecular tumbling time (see below) (Lee et al. 2000; Mittermaier et al. 1999). This method can also be used for weak complexes in which ligand binding is characterized by fast exchange. As the titration of weak binding ligands can connect the methionine assignments in unbound CaM to those in the complex, the limiting factor would become the collection of intermolecular NOEs a condition potentially overcome by super-saturating the system. As a final note, it is possible that a complex structure could be further improved by labeling additional side chains, other methyl groups or aromatics, however, this process is quite laborious and due to the strategic positioning of the methionine probes the improved structural accuracy may not be that considerable.

Finally, the advantages of methyl-labeled deuterated methionine can be extended beyond the method presented here. First, as the remaining aliphatic carbons are attached to deuterium, collecting and analyzing NOEs between the methyl group and a bound ligand is quite straightforward. This has direct application for other systems in which methionine side chains play an important role in ligand binding. For example, this method could be employed in structural studies examining both protein ligand and drug binding to troponin C (Lin et al. 1994; Kleerekoper and Putkey 1999) or the binding of ER-destined nascent peptide chains to the SRP45 subunit of the signal recognition particle (Grudnik et al. 2009) as both proteins are also methionine rich. Secondly, thanks to the intrinsic detection sensitivity of the methyl group, the significant degree of internal mobility normally observed for this amino acid and its relatively low abundance, the use of the methyl group of methionine to probe dynamics, conformation, and ligand binding even in large proteins has become popular. To date a number of large proteins/complexes have been studied through methyl-labeled methionine including UvrB (75 kDa) (DellaVecchia et al. 2007), transferrin (80 kDa) (He et al. 1999; Beatty et al. 1996), HIV-1 reverse transcriptase (117 kDa) (Zheng et al. 2009, 2010), the proteasome (180 kDa) (Religa et al. 2010) and SecA (204 kDa) (Gelis et al. 2007). To the best of our knowledge, this work has been performed using completely protonated methionine (^{13}C-ε-methionine). Due to the deuteration of the aliphatic carbons, the methyl-labeled methionine used in this study (^{1}H-α,ε- ^{13}C-ε- ^{2}H-methionine) has more desirable relaxation characteristics enabling high-quality methionine methyl-TROSY spectra to be recorded.

Acknowledgments The authors wish to thank Deane D. McIntyre for the synthesis of (^{1}H-α,ε- ^{13}C-ε- ^{2}H-methionine) as well as for spectrometer maintenance, Renee Otten for helpful discussions, and the Canadian Institutes of Health Research for operating support. J.L.G. is the recipient of postgraduate scholarships from the National Science and Engineering Research Council and Alberta Ingenuity Fund as well as a Killam Fellowship. H.J.V. is an Alberta Heritage Foundation for Medical Research Scientist.

References

Barbato G, Ikura M, Kay LE, Pastor RW, Bax A (1992) Backbone dynamics of calmodulin studied by 15N relaxation using inverse detected two-dimensional NMR spectroscopy: the central helix is flexible. Biochemistry 31(23):5269–5278

Barth A, Martin SR, Bayley PM (1998) Resolution of Trp near UV CD spectra of calmodulin-domain peptide complexes into the 1La and 1Lb component spectra. Biopolymers 45(7):493–501. doi:10.1002/(SICI)1097-0282(199806)45:7<493:AID-BIP3>3.0.CO;2-J

Bax A, Delaglio F, Grzesiek S, Vuister GW (1994) Resonance assignment of methionine methyl groups and chi 3 angular information from long-range proton-carbon and carbon-carbon J correlation in a calmodulin-peptide complex. J Biomol NMR 4(6):787–797

Beatty EJ, Cox MC, Frenkiel TA, Tam BM, Mason AB, MacGillivray RT, Sadler PJ, Woodworth RC (1996) Interlobe communication in 13C-methionine-labeled human transferrin. Biochemistry 35(24):7635–7642. doi:10.1021/bi960684g

Breeze AL (2000) Isotope-filtered NMR methods for the study of biomolecular structure and interactions. Prog Nucl Magn Reson Spectrosc 36(4):323–372

Chin D, Means AR (1996) Methionine to glutamine substitutions in the C-terminal domain of calmodulin impair the activation of three protein kinases. J Biol Chem 271(48):30465–30471

Chin D, Means AR (2000) Calmodulin: a prototypical calcium sensor. Trends Cell Biol 10(8):322–328. doi:S0962-8924(00)01800-6

Chin D, Sloan DJ, Quiocho FA, Means AR (1997) Functional consequences of truncating amino acid side chains located at a calmodulin-peptide interface. J Biol Chem 272(9):5510–5513

Chou JJ, Li S, Bax A (2000) Study of conformational rearrangement and refinement of structural homology models by the use of heteronuclear dipolar couplings. J Biomol NMR 18(3):217–227

Clapperton JA, Martin SR, Smerdon SJ, Gamblin SJ, Bayley PM (2002) Structure of the complex of calmodulin with the target sequence of calmodulin-dependent protein kinase I: studies of the kinase activation mechanism. Biochemistry 41(50):14669–14679. doi:bi026660t

Contessa GM, Orsale M, Melino S, Torre V, Paci M, Desideri A, Cicero DO (2005) Structure of calmodulin complexed with an olfactory CNG channel fragment and role of the central linker: residual dipolar couplings to evaluate calmodulin binding modes outside the kinase family. J Biomol NMR 31(3):185–199. doi:10.1007/s10858-005-0165-1

Cornilescu G, Delaglio F, Bax A (1999) Protein backbone angle restraints from searching a database for chemical shift and sequence homology. J Biomol NMR 13(3):289–302

Davis TN, Urdea MS, Masiarz FR, Thorner J (1986) Isolation of the yeast calmodulin gene: calmodulin is an essential protein. Cell 47(3):423–431. doi:0092-8674(86)90599-4

Delaglio F, Grzesiek S, Vuister GW, Zhu G, Pfeifer J, Bax A (1995) NMRPipe: a multidimensional spectral processing system based on UNIX pipes. J Biomol NMR 6(3):277–293

DellaVecchia MJ, Merritt WK, Peng Y, Kirby TW, DeRose EF, Mueller GA, Van Houten B, London RE (2007) NMR analysis of [methyl-13C]methionine UvrB from Bacillus caldotenax reveals UvrB-domain 4 heterodimer formation in solution. J Mol Biol 373(2):282–295. doi:10.1016/j.jmb.2007.07.045

Edwards RA, Walsh MP, Sutherland C, Vogel HJ (1998) Activation of calcineurin and smooth muscle myosin light chain kinase by Met-to-Leu mutants of calmodulin. Biochem J 331(Pt 1):149–152

Gelis I, Bonvin AM, Keramisanou D, Koukaki M, Gouridis G, Karamanou S, Economou A, Kalodimos CG (2007) Structural basis for signal-sequence recognition by the translocase motor SecA as determined by NMR. Cell 131(4):756–769. doi:10.1016/j.cell.2007.09.039

Gellman SH (1991) On the role of methionine residues in the sequence-independent recognition of nonpolar protein surfaces. Biochemistry 30(27):6633–6636

Gifford JL, Walsh MP, Vogel HJ (2007) Structures and metal-ion-binding properties of the Ca2+-binding helix-loop-helix EF-hand motifs. Biochem J 405(2):199–221. doi:10.1042/BJ20070255

Goldberg J, Nairn AC, Kuriyan J (1996) Structural basis for the autoinhibition of calcium/calmodulin-dependent protein kinase I. Cell 84(6):875–887. doi:S0092-8674(00)81066-1

Gomes AV, Barnes JA, Vogel HJ (2000) Spectroscopic characterization of the interaction between calmodulin-dependent protein kinase I and calmodulin. Arch Biochem Biophys 379(1):28–36. doi:10.1006/abbi.2000.1827

Grudnik P, Bange G, Sinning I (2009) Protein targeting by the signal recognition particle. Biol Chem 390(8):775–782. doi:10.1515/BC.2009.102

Guntert P (2003) Automated NMR protein structure calculation. Prog Nucl Magn Reson Spectrosc 43(3–4):105–125. doi:10.1016/S0079-6565(03)00021-9

He QY, Mason AB, Tam BM, MacGillivray RT, Woodworth RC (1999) [13C]Methionine NMR and metal-binding studies of recombinant human transferrin N-lobe and five methionine mutants: conformational changes and increased sensitivity to chloride. Biochem J 344(Pt 3):881–887

Hoeflich KP, Ikura M (2002) Calmodulin in action: diversity in target recognition and activation mechanisms. Cell 108(6):739–742. doi:S0092867402006827

Ishida H, Vogel HJ (2006) Protein-peptide interaction studies demonstrate the versatility of calmodulin target protein binding. Protein Pept Lett 13(5):455–465

Johnson BA, Blevins RA (1994) Nmr view—a computer-program for the visualization and analysis of Nmr data. J Biomol NMR 4(5):603–614

Kleerekoper Q, Putkey JA (1999) Drug binding to cardiac troponin C. J Biol Chem 274(34):23932–23939

Koradi R, Billeter M, Wuthrich K (1996) MOLMOL: a program for display and analysis of macromolecular structures. J Mol Graph 14(1):51–55, 29–32

Kranz JK, Lee EK, Nairn AC, Wand AJ (2002) A direct test of the reductionist approach to structural studies of calmodulin activity: relevance of peptide models of target proteins. J Biol Chem 277(19):16351–16354. doi:10.1074/jbc.C200139200

Krueger JK, Olah GA, Rokop SE, Zhi G, Stull JT, Trewhella J (1997) Structures of calmodulin and a functional myosin light chain kinase in the activated complex: a neutron scattering study. Biochemistry 36(20):6017–6023. doi:10.1021/bi9702703

Lee AL, Kinnear SA, Wand AJ (2000) Redistribution and loss of side chain entropy upon formation of a calmodulin-peptide complex. Nat Struct Biol 7(1):72–77. doi:10.1038/71280

Lin X, Krudy GA, Howarth J, Brito RM, Rosevear PR, Putkey JA (1994) Assignment and calcium dependence of methionyl epsilon C and epsilon H resonances in cardiac troponin C. Biochemistry 33(48):14434–14442

Mal TK, Skrynnikov NR, Yap KL, Kay LE, Ikura M (2002) Detecting protein kinase recognition modes of calmodulin by residual dipolar couplings in solution NMR. Biochemistry 41(43):12899–12906. doi:bi0264162

Melville DB, Rachele JR, Keller EB (1947) A synthesis of methionine containing radiocarbon in the methyl group. J Biol Chem 169(2):419–426

Mittermaier A, Kay LE, Forman-Kay JD (1999) Analysis of deuterium relaxation-derived methyl axis order parameters and

correlation with local structure. J Biomol NMR 13(2):181–185. doi:10.1023/A:1008387715167
Morris AL, MacArthur MW, Hutchinson EG, Thornton JM (1992) Stereochemical quality of protein structure coordinates. Proteins 12(4):345–364. doi:10.1002/prot.340120407
Osawa M, Tokumitsu H, Swindells MB, Kurihara H, Orita M, Shibanuma T, Furuya T, Ikura M (1999) A novel target recognition revealed by calmodulin in complex with Ca2+-calmodulin-dependent kinase kinase. Nat Struct Biol 6(9):819–824. doi:10.1038/12271
Otten R, Chu B, Krewulak KD, Vogel HJ, Mulder FA (2010) Comprehensive and cost-effective NMR spectroscopy of methyl groups in large proteins. J Am Chem Soc 132(9):2952–2960. doi:10.1021/ja907706a
Ottiger M, Delaglio F, Bax A (1998) Measurement of J and dipolar couplings from simplified two-dimensional NMR spectra. J Magn Reson 131(2):373–378. doi:10.1006/jmre.1998.1361
Religa TL, Sprangers R, Kay LE (2010) Dynamic regulation of archaeal proteasome gate opening as studied by TROSY NMR. Science 328(5974):98–102. doi:10.1126/science.1184991
Ruschak AM, Kay LE (2010) Methyl groups as probes of supramolecular structure, dynamics and function. J Biomol NMR 46(1):75–87. doi:10.1007/s10858-009-9376-1
Scheschonka A, Findlow S, Schemm R, El Far O, Caldwell JH, Crump MP, Holden-Dye K, O'Connor V, Betz H, Werner JM (2008) Structural determinants of calmodulin binding to the intracellular C-terminal domain of the metabotropic glutamate receptor 7A. J Biol Chem 283(9):5577–5588. doi:10.1074/jbc.M709505200
Schwieters CD, Kuszewski JJ, Tjandra N, Clore GM (2003) The Xplor-NIH NMR molecular structure determination package. J Magn Reson 160(1):65–73. doi:S1090-7807(02)00014-9
Siivari K, Zhang M, Palmer AG 3rd, Vogel HJ (1995) NMR studies of the methionine methyl groups in calmodulin. FEBS Lett 366(2–3):104–108. doi:0014-5793(95)00504-3
Soderling TR (1999) The Ca-calmodulin-dependent protein kinase cascade. Trends Biochem Sci 24(6):232–236. doi:S0968000499013833
Tjandra N, Kuboniwa H, Ren H, Bax A (1995) Rotational dynamics of calcium-free calmodulin studied by 15N-NMR relaxation measurements. Eur J Biochem 230(3):1014–1024
Tjandra N, Omichinski JG, Gronenborn AM, Clore GM, Bax A (1997) Use of dipolar 1H–15N and 1H–13C couplings in the structure determination of magnetically oriented macromolecules in solution. Nat Struct Biol 4(9):732–738
Tugarinov V, Kanelis V, Kay LE (2006) Isotope labeling strategies for the study of high-molecular-weight proteins by solution NMR spectroscopy. Nat Protoc 1(2):749–754. doi:10.1038/nprot.2006.101
Vogel HJ (1994) The Merck Frosst award lecture 1994. Calmodulin: a versatile calcium mediator protein. Biochem Cell Biol 72(9–10):357–376
Wayman GA, Lee YS, Tokumitsu H, Silva AJ, Soderling TR (2008) Calmodulin-kinases: modulators of neuronal development and plasticity. Neuron 59(6):914–931. doi:10.1016/j.neuron.2008.08.021
Wishart DS, Bigam CG, Yao J, Abildgaard F, Dyson HJ, Oldfield E, Markley JL, Sykes BD (1995) 1H, 13C and 15N chemical shift referencing in biomolecular NMR. J Biomol NMR 6(2):135–140
Yamniuk AP, Vogel HJ (2004) Calmodulin's flexibility allows for promiscuity in its interactions with target proteins and peptides. Mol Biotechnol 27(1):33–57. doi:10.1385/MB:27:1:33
Yamniuk AP, Ishida H, Lippert D, Vogel HJ (2009) Thermodynamic effects of noncoded and coded methionine substitutions in calmodulin. Biophys J 96(4):1495–1507. doi:10.1016/j.bpj.2008.10.060
Yap KL, Kim J, Truong K, Sherman M, Yuan T, Ikura M (2000) Calmodulin target database. J Struct Funct Genomics 1(1):8–14
Yuan T, Weljie AM, Vogel HJ (1998) Tryptophan fluorescence quenching by methionine and selenomethionine residues of calmodulin: orientation of peptide and protein binding. Biochemistry 37(9):3187–3195. doi:10.1021/bi9716579
Yuan T, Ouyang H, Vogel HJ (1999) Surface exposure of the methionine side chains of calmodulin in solution. A nitroxide spin label and two-dimensional NMR study. J Biol Chem 274(13):8411–8420
Yuan T, Gomes AV, Barnes JA, Hunter HN, Vogel HJ (2004) Spectroscopic characterization of the calmodulin-binding and autoinhibitory domains of calcium/calmodulin-dependent protein kinase I. Arch Biochem Biophys 421(2):192–206
Zhang M, Vogel HJ (1993) Determination of the side chain pKa values of the lysine residues in calmodulin. J Biol Chem 268(30):22420–22428
Zhang M, Vogel HJ (1994) Two-dimensional NMR studies of selenomethionyl calmodulin. J Mol Biol 239(4):545–554. doi:10.1006/jmbi.1994.1393
Zhang M, Li M, Wang JH, Vogel HJ (1994) The effect of Met–>Leu mutations on calmodulin's ability to activate cyclic nucleotide phosphodiesterase. J Biol Chem 269(22):15546–15552
Zhang M, Tanaka T, Ikura M (1995) Calcium-induced conformational transition revealed by the solution structure of apo calmodulin. Nat Struct Biol 2(9):758–767
Zheng X, Mueller GA, DeRose EF, London RE (2009) Solution characterization of [methyl-(13)C]methionine HIV-1 reverse transcriptase by NMR spectroscopy. Antiviral Res 84(3):205–214. doi:10.1016/j.antiviral.2009.07.021
Zheng X, Mueller GA, Cuneo MJ, Derose EF, London RE (2010) Homodimerization of the p51 subunit of HIV-1 reverse transcriptase. Biochemistry 49(13):2821–2833. doi:10.1021/bi902116z
Zweckstetter M, Bax A (2000) Prediction of sterically induced alignment in a dilute liquid crystalline phase: aid to protein structure determination by NMR. J Am Chem Soc 122(15):3791–3792